References

Amaral AI (2012) Effects of hypoglycaemia on neuronal metabolism in the adult brain: role of alternative substrates to glucose. J Inherit Metab Dis. doi:10.1007/s10545-012-9553-3

Antonicka H, Ostergaard E, Sasarman F, Weraarpachai W, Wibrand F, Pedersen AM, Rodenburg RJ, van der Knaap MS, Smeitink JA, Chrzanowska-Lightowlers ZM, Shoubridge EA (2010) Mutations in C12orf65 in patients with encephalomyopathy and a mitochondrial translation defect. Am J Hum Genet 87:115–122. doi:10.1016/j.ajhg.2010.06.004

Barbetti F, Rocchi M, Bossolasco M, Cordera R, Sbraccia P, Finelli P, Consalez GG (1996) The human skeletal muscle glycogenin gene: cDNA, tissue expression and chromosomal localization. Biochem Biophys Res Commun 220:72–77. doi:10.1006/bbrc.1996.0359

Benke PJ, Parker JC Jr, Lubs ML, Benkendorf J, Feuer AE (1982) X-linked Leigh's syndrome. Hum Genet 62:52–59

Bollen M, Keppens S, Stalmans W (1998) Specific features of glycogen metabolism in the liver. Biochem J 336:19–31

Brown GK, Squier MV (1996) Neuropathology and pathogenesis of mitochondrial diseases. J Inherit Metab Dis 19:553–572

Cao Y, Mahrenholz AM, DePaoli-Roach AA, Roach PJ (1993) Characterization of rabbit skeletal muscle glycogenin. Tyrosine 194 is essential for function. J Biol Chem 268:14687–14693

Chaikuad A, Froese DS, Berridge G, von Delft F, Oppermann U, Yue WW (2011) Conformational plasticity of glycogenin and its maltosaccharide substrate during glycogen biogenesis. Proc Natl Acad Sci USA 108:21028–21033. doi:10.1073/pnas.1113921108

Debray FG, Morin C, Janvier A, Villeneuve J, Maranda B, Laframboise R, Lacroix J, Decarie JC, Robitaille Y, Lambert M, Robinson BH, Mitchell GA (2011) LRPPRC mutations cause a phenotypically distinct form of Leigh syndrome with cytochrome c oxidase deficiency. J Med Genet 48:183–189. doi:10.1136/jmg.2010.081976

Farina L, Chiapparini L, Uziel G, Bugiani M, Zeviani M, Savoiardo M (2002) MR findings in Leigh syndrome with COX deficiency and SURF-1 mutations. AJNR Am J Neuroradiol 23:1095–1100

Finsterer J (2008) Leigh and Leigh-like syndrome in children and adults. Pediatr Neurol 39:223–235. doi:10.1016/j.pediatrneurol.2008.07.013

Garber AJ, Menzel PH, Boden G, Owen OE (1974) Hepatic ketogenesis and gluconeogenesis in humans. J Clin Invest 54:981–989. doi:10.1172/JCI107839

Gibbons BJ, Roach PJ, Hurley TD (2002) Crystal structure of the autocatalytic initiator of glycogen biosynthesis, glycogenin. J Mol Biol 319:463–477. doi:10.1016/S0022-2836(02)00305-4

Guerois R, Nielsen JE, Serrano L (2002) Predicting changes in the stability of proteins and protein complexes: a study of more than 1000 mutations. J Mol Biol 320:369–387. doi:10.1016/S0022-2836(02)00442-4

Khan S, Vihinen M (2010) Performance of protein stability predictors. Hum Mutat 31:675–684. doi:10.1002/humu.21242

Krisman CR, Barengo R (1975) A precursor of glycogen biosynthesis: alpha-1,4-glucan-protein. Eur J Biochem 52:117–123

Laffel L (1999) Ketone bodies: a review of physiology, pathophysiology and application of monitoring to diabetes. Diabetes Metab Res Rev 15:412–426

Larner J (1953) The action of branching enzymes on outer chains of glycogen. J Biol Chem 202:491–503

Leigh D (1951) Subacute necrotizing encephalomyelopathy in an infant. J Neurol Neurosurg Psychiatry 14:216–221

Lomako J, Lomako WM, Whelan WJ (1988) A self-glucosylating protein is the primer for rabbit muscle glycogen biosynthesis. FASEB J 2:3097–3103

Lomako J, Lomako WM, Whelan WJ (2004) Glycogenin: the primer for mammalian and yeast glycogen synthesis. Biochim Biophys Acta 1673:45–55. doi:10.1016/j.bbagen.2004.03.017

Lopez LC, Schuelke M, Quinzii CM, Kanki T, Rodenburg RJ, Naini A, Dimauro S, Hirano M (2006) Leigh syndrome with nephropathy and CoQ10 deficiency due to decaprenyl diphosphate synthase subunit 2 (PDSS2) mutations. Am J Hum Genet 79:1125–1129. doi:10.1086/510023

Magistretti PJ, Pellerin L (1999) Cellular mechanisms of brain energy metabolism and their relevance to functional brain imaging. Philos Trans R Soc Lond B Biol Sci 354:1155–1163. doi:10.1098/rstb.1999.0471

Martin MA, Blazquez A, Gutierrez-Solana LG, Fernandez-Moreira D, Briones P, Andreu AL, Garesse R, Campos Y, Arenas J (2005) Leigh syndrome associated with mitochondrial complex I deficiency due to a novel mutation in the NDUFS1 gene. Arch Neurol 62:659–661. doi:10.1001/archneur.62.4.659

Medina L, Chi TL, DeVivo DC, Hilal SK (1990) MR findings in patients with subacute necrotizing encephalomyelopathy (Leigh syndrome): correlation with biochemical defect. AJR Am J Roentgenol 154:1269–1274

Moslemi AR, Lindberg C, Nilsson J, Tajsharghi H, Andersson B, Oldfors A (2010) Glycogenin-1 deficiency and inactivated priming of glycogen synthesis. N Engl J Med 362:1203–1210. doi:10.1056/NEJMoa0900661

Mu J, Roach PJ (1998) Characterization of human glycogenin-2, a self-glucosylating initiator of liver glycogen metabolism. J Biol Chem 273:34850–34856

Mu J, Skurat AV, Roach PJ (1997) Glycogenin-2, a novel self-glucosylating protein involved in liver glycogen biosynthesis. J Biol Chem 272:27589–27597

Naess K, Freyer C, Bruhn H, Wibom R, Malm G, Nennesmo I, von Dobeln U, Larsson NG (2009) MtDNA mutations are a common cause of severe disease phenotypes in children with Leigh syndrome. Biochim Biophys Acta 1787:484–490. doi:10.1016/j.bbabio.2008.11.014

Ostergaard E, Hansen FJ, Sorensen N, Duno M, Vissing J, Larsen PL, Faeroe O, Thorgrimsson S, Wibrand F, Christensen E, Schwartz M (2007) Mitochondrial encephalomyopathy with elevated methylmalonic acid is caused by SUCLA2 mutations. Brain 130:853–861. doi:10.1093/brain/awl383

Picardi E, Pesole G (2012) Mitochondrial genomes gleaned from human whole-exome sequencing. Nat Methods 9:523–524. doi:10.1038/nmeth.2029

Pitcher J, Smythe C, Cohen P (1988) Glycogenin is the priming glucosyltransferase required for the initiation of glycogen biogenesis in rabbit skeletal muscle. Eur J Biochem 176:391–395

Quinonez SC, Leber SM, Martin DM, Thoene JG, Bedoyan JK (2013) Leigh syndrome in a girl with a novel DLD mutation causing E3 deficiency. Pediatr Neurol 48:67–72. doi:10.1016/j.pediatrneurol.2012.09.013

Rahman S, Blok RB, Dahl HH, Danks DM, Kirby DM, Chow CW, Christodoulou J, Thorburn DR (1996) Leigh syndrome: clinical features and biochemical and DNA abnormalities. Ann Neurol 39:343–351. doi:10.1002/ana.410390311

Randle PJ, Newsholme EA, Garland PB (1964) Regulation of glucose uptake by muscle. 8. Effects of fatty acids, ketone bodies and pyruvate, and of alloxan-diabetes and starvation, on the uptake and metabolic fate of glucose in rat heart and diaphragm muscles. Biochem J 93:652–665

Smythe C, Caudwell FB, Ferguson M, Cohen P (1988) Isolation and structural analysis of a peptide containing the novel tyrosyl-glucose linkage in glycogenin. EMBO J 7:2681–2686

van Erven PM, Cillessen JP, Eekhoff EM, Gabreels FJ, Doesburg WH, Lemmens WA, Slooff JL, Renier WO, Ruitenbeek W (1987)

Leigh syndrome, a mitochondrial encephalo(myo)pathy. A review of the literature. Clin Neurol Neurosurg 89:217–230

Viskupic E, Cao Y, Zhang W, Cheng C, DePaoli-Roach AA, Roach PJ (1992) Rabbit skeletal muscle glycogenin. Molecular cloning and production of fully functional protein in Escherichia coli. J Biol Chem 267:25759–25763

Zhai L, Schroeder J, Skurat AV, Roach PJ (2001) Do rodents have a gene encoding glycogenin-2, the liver isoform of the self-glucosylating initiator of glycogen synthesis? IUBMB Life 51:87–91. doi:10.1080/15216540117315

Brachial plexus MRI showed increased signal intensity with contrast enhancement of the right long thoracic nerve, suggesting inflammation (Fig. 1). The patient was given oral prednisolone, 1 mg/kg daily for 21 days, with dose tapering over the next month. Three months later, her symptoms were stable, but electrophysiological follow-up showed a slight reduction of fibrillation potentials in right serratus anterior muscle.

Scapular winging is caused by imbalanced action of scapular muscles. The clinical examination based on the muscle group affected (trapezius, rhomboids, serratus anterior) is still the first guide for interpretation both of "pure" and "complicated" phenotypes.[1] Isolated scapular winging due to serratus anterior weakness is usually caused by traumatic or postsurgical long thoracic nerve injury, or it can occur as a manifestation of neuralgic amyotrophy, also known as Parsonage-Turner syndrome (PTS). PTS is a clinical syndrome characterized by attacks of extreme pain at onset, patchy weakness in the upper extremities, and atrophy of affected muscles.[2]

The available evidence suggests that PTS has a complex pathophysiology that includes an underlying predisposition, susceptibility to dysfunction of some peripheral nervous system structures, and an autoimmune trigger.[3] Cases of PTS are described after an immune event, such as pregnancy, childbirth, vaccination, or infection.[2]

Our patient did not have a history of previous surgery or trauma involving the thoracic area. Other possible causes were excluded by the laboratory evaluation. Moreover, she did not experience acute pain at onset, but only subsequent musculoskeletal pain due to compensation for the deficit. Since childbirth, an immunological trigger, occurred 3 days before symptom onset and approximately 4% of patients with PTS do not experience pain,[2] we made a diagnosis of post-partum PTS.

Currently, neuralgic amyotrophy cannot be diagnosed confidently by a single test, and often the presence of extreme pain of the upper limb together with patchy paresis helps in the diagnosis. In PTS without pain at onset, neuroimaging studies can be very useful, because they can exclude other causes such as intervertebral disc disease, tumors, or entrapment neuropathies. Furthermore, the evidence of contrast enhancement on MRI suggests a possible inflammatory etiology, thus supporting early administration of corticosteroids even in absence of pain, to block further evolution of the clinical picture and to possibly speed up functional nerve recovery.

In conclusion, contrast-enhanced MRI can provide crucial help in identifying different phenotypes of PTS and can guide therapy.

Viviana Nociti, MD, PhD[1]
Mauro Monforte, MD,[2]
Alessia Perna, MD[2]
Francesca Madia, MD, PhD[2]
Giovanni Melchiorri, MD[3]
Massimiliano Mirabella, MD, PhD[2]

[1]Don Carlo Gnocchi Onlus Foundation, Milan, Italy

[2]Institute of Neurology, Catholic University, Rome, Italy

[3]Motor Science Degree, Tor Vergata University, Rome, Italy

1. Monforte M, Ricci E, Iannaccone E, Tasca G. Teaching Video NeuroImages: Complicated scapular winging. Neurology 2013;81:e95.
2. van Alfen N. Clinical and pathophysiological concepts of neuralgic amyotrophy. Nat Rev Neurol 2011;7:315–322.
3. van Alfen N. The neuralgic amyotrophy consultation. J Neurol 2007; 254:695–704.

Published online 13 September 2013 in Wiley Online Library (wileyonlinelibrary.com). DOI 10.1002/mus.24073

A PRIMIGRAVIDA WITH VERY-LONG-CHAIN ACYL-CoA DEHYDROGENASE DEFICIENCY

We report a woman who had the adult-onset form of very-long-chain acyl-CoA dehydrogenase (VLCAD) deficiency[1,2] and developed acute postpartum heart failure due to cardiomyopathy.

A 34-year-old primigravida visited our clinic due to nocturnal dyspnea. She had suffered from exercise-induced muscle pain since she was 5 years of age. Her food intake was insufficient due to hyperemesis gravidarum, and she developed severe generalized myalgia at 14 weeks' gestation. Her serum creatine kinase was 21,530 IU/L, and myoglobinuria was detected. From 15–30 weeks' gestation, her appetite recovered, and frequency of myalgia decreased. She delivered a baby by Caesarean section at 37 weeks without any complications.

She was transferred to our hospital on postpartum day 10 for treatment of heart failure. Serum glucose, creatine kinase, lactate, pyruvate, ammonia, and cardiac troponin T were within the normal ranges, but brain natriuretic peptide was increased to 3194.5 pg/ml. The left ventricular ejection fraction on echocardiography was 30%. Furosemide and carperitide were administered intravenously, and oral losartan and carvedilol were started on day 6 after admission. Sixty days after admission, echocardiography revealed no pericardial effusion and normal movement of the basal portion of the septum without any medications. There was no muscle weakness during or after pregnancy.

A muscle biopsy showed only mild fiber size variation without pathological findings. We measured acyl-CoA dehydrogenase activities using frozen muscle biopsy specimens.[3] Palmitoyl-CoA activity was reduced

Table 1. Results of β-oxidation enzyme analysis.

	Patient	Controls
Carnitine (free)	3.7	12.9 ± 3.7
Carnitine (total)	5.8	15.7 ± 2.8
Carnitine palmytoyl transferase II	0.9	1.6 ± 0.4
Acyl-CoA-dehydrogenase (substrate: C16:0)	4.1	24.5 ± 6.1
Acyl-CoA-dehydrogenase (substrate: C8:0)	6.1	8.1 ± 2.5
Acyl-CoA-dehydrogenase (substrate: C4:0)	15.7	16.8 ± 3.9
C16:0/C8:0	0.7	3.8 ± 1.4
C16:0/C4:0	0.3	1.8 ± 0.2
C8:0/C4:0	0.4	0.5 ± 0.1

compared with normal controls, but octanoyl-CoA activity was within the normal range (Table 1).

We sequenced the acyl-CoA dehydrogenase (very-long-chain) (*ACADVL*) gene in both the patient and controls.[4,5] DNA was extracted from muscle biopsy specimens using conventional methods. Sequence analysis of *ACADVL* revealed a novel homozygous c.272C>T mutation (p.P91L).

Patients with missense mutations or single amino acid deletions in the adult-onset form of VLCAD deficiency show energy deficiency and exercise-induced rhabdomyolysis or myoglobinuria.[6,7] During early pregnancy, our patient was malnourished due to hyperemesis gravidarum and suffered severe myalgia and rhabdomyolysis. She also developed acute heart failure at 2 weeks postpartum. She lacked the capacity for proper fatty acid oxidation and was in a catabolic state. In addition to a poor nutritional state, delivery may have served as a trigger for acute energy failure.

The nature of heart failure in our patient is quite different from that of rhabdomyolysis. Because Ca^{2+} homeostasis is altered in the VLCAD$^{-/-}$ mouse heart, abnormal intracellular Ca^{2+} handling can cause arrhythmias and lethal cardiac failure.[8] The accumulation of long-chain acylcarnitines in the heart has been shown to lead to cardiomyopathy and arrhythmia due to calcium uncoupling disorders.[9] Although cardiomyopathy has been reported in the childhood form of severe VLCAD deficiency,[10] 13% of patients with adult-onset VLCAD deficiency also develop cardiomyopathy.[6,11] Unlike the childhood form, patients with the adult-onset form due to missense mutations or single amino acid deletions have slight residual VLCAD activity and can avoid severe heart failure when treated with medium-chain triglycerides as the major source of dietary fat.[12,13] VLCAD deficiency should be included in the differential diagnosis of acute postpartum cardiomyopathy.

Ken-ya Murata, MD, PhD[1]
Hideo Sugie, MD, PhD[2]
Ichizo Nishino, MD, PhD[3]
Tomoyoshi Kondo, MD, PhD[1]
Hidefumi Ito, MD, PhD[1]

[1]Department of Neurology, Wakayama Medical University, Wakayama, Japan

[2]Department of Pediatrics, Jichi Medical University, Tochigi, Japan

[3]Department of Neuromuscular Research, National Institute of Neuroscience, National Center for Neurology and Psychiatry, Tokyo, Japan

1. Pons R, Cavadini P, Baratta S, Invernizzi F, Lamantea E, Garavaglia B, et al. Clinical and molecular heterogeneity in very-long-chain acyl-coenzyme A dehydrogenase deficiency. Pediatr Neurol 2000;22:98–105.
2. Izai K, Uchida Y, Orii T, Yamamoto S, Hashimoto T. Novel fatty acid beta-oxidation enzymes in rat liver mitochondria. I. Purification and properties of very-long-chain acyl-coenzyme A dehydrogenase. J Biol Chem 1992;267:1027–1033.
3. Verity MA, Turnbull DM. Assay of acyl-CoA dehydrogenase activity in frozen muscle biopsies: application to medium-chain acyl-CoA dehydrogenase deficiency. Biochem Med Metab Biol 1993;49:351–362.
4. Andresen BS, Bross P, Vianey-Saban C, Divry P, Zabot MT, Roe CR, et al. Cloning and characterization of human very-long-chain acyl-CoA dehydrogenase cDNA, chromosomal assignment of the gene and identification in four patients of nine different mutations within the VLCAD gene. Hum Mol Genet 1996;5:461–472.
5. Orii KO, Aoyama T, Souri M, Orii KE, Kondo N, Orii T, et al. Genomic DNA organization of human mitochondrial very-long-chain acyl-CoA dehydrogenase and mutation analysis. Biochem Biophys Res Commun 1995;217:987–992.
6. Andresen BS, Olpin S, Poorthuis BJ, Scholte HR, Vianey-Saban C, Wanders R, et al. Clear correlation of genotype with disease phenotype in very-long-chain acyl-CoA dehydrogenase deficiency. Am J Hum Genet 1999;64:479–494.
7. Orngreen MC, Norgaard MG, Sacchetti M, van Engelen BG, Vissing J. Fuel utilization in patients with very long-chain acyl-CoA dehydrogenase deficiency. Ann Neurol 2004;56:279–283.
8. Werdich AA, Baudenbacher F, Dzhura I, Jeyakumar LH, Kannankeril PJ, Fleischer S, et al. Polymorphic ventricular tachycardia and abnormal $Ca2^{+}$ handling in very-long-chain acyl-CoA dehydrogenase null mice. Am J Physiol Heart Circ Physiol 2007;292:H2202–2211.
9. Yamada KA, McHowat J, Yan GX, Donahue K, Peirick J, Kleber AG, et al. Cellular uncoupling induced by accumulation of long-chain acylcarnitine during ischemia. Circ Res 1994;74:83–95.
10. Yamaguchi S, Indo Y, Coates PM, Hashimoto T, Tanaka K. Identification of very-long-chain acyl-CoA dehydrogenase deficiency in three patients previously diagnosed with long-chain acyl-CoA dehydrogenase deficiency. Pediatr Res 1993;34:111–113.
11. Parini R, Menni F, Garavaglia B, Fesslova V, Melotti D, Massone ML, et al. Acute, severe cardiomyopathy as main symptom of late-onset very long-chain acyl-coenzyme A dehydrogenase deficiency. Eur J Pediatr 1998;157:992–995.
12. Brown-Harrison MC, Nada MA, Sprecher H, Vianey-Saban C, Farquhar J Jr, Gilladoga AC, et al. Very long chain acyl-CoA dehydrogenase deficiency: successful treatment of acute cardiomyopathy. Biochem Mol Med 1996;58:59–65.
13. Bhattacharyya A, Basra SS, Sen P, Kar B. Peripartum cardiomyopathy: a review. Tex Heart Inst J 2012;39:8–16.

Published online 22 August 2013 in Wiley Online Library (wileyonlinelibrary.com). DOI 10.1002/mus.24055

Available online at www.sciencedirect.com

SciVerse ScienceDirect

Neuromuscular Disorders 22 (2012) 389–393

www.elsevier.com/locate/nmd

Case report

Acid phosphatase-positive globular inclusions is a good diagnostic marker for two patients with adult-onset Pompe disease lacking disease specific pathology

Rie S. Tsuburaya [a,b], Kazunari Monma [a], Yasushi Oya [a], Takahiro Nakayama [c], Tokiko Fukuda [d], Hideo Sugie [d], Yukiko K. Hayashi [a], Ikuya Nonaka [a], Ichizo Nishino [a,*]

[a] *Department of Neuromuscular Research, National Institute of Neuroscience, National Center of Neurology and Psychiatry, Kodaira, Tokyo, Japan*
[b] *Department of Pediatrics, Tohoku University School of Medicine, Miyagi, Japan*
[c] *Department of Neurology, Yokohama Rosai Hospital, Kanagawa, Japan*
[d] *Department of Pediatrics, Jichi Medical University and Jichi Children's Medical Center, Tochigi, Japan*

Received 18 August 2011; received in revised form 19 October 2011; accepted 15 November 2011

Abstract

Diagnosis of adult-onset Pompe disease is sometimes challenging because of its clinical similarities to muscular dystrophy and the paucity of disease-specific vacuolated fibers in the skeletal muscle pathology. We describe two patients with adult-onset Pompe disease whose muscle pathology showed no typical vacuolated fibers but did show unique globular inclusions with acid phosphatase activity. The acid phosphatase-positive globular inclusions may be a useful diagnostic marker for adult-onset Pompe disease even when typical vacuolated fibers are absent.

Keywords: Pompe disease; *GAA*; Globular inclusion; Acid phosphatase

1. Introduction

Pompe disease (glycogen storage disease type 2; acid maltase deficiency; OMIM #232300) is an autosomal recessive disease caused by mutations in the gene encoding acid α-glucosidase (GAA, OMIM #606800), a lysosomal enzyme involved in glycogen degradation [1]. Based on age of onset and clinical severity, which depends on residual GAA activity, the disease can be classified into infantile, childhood-onset, and adult-onset forms.

Most of the infantile and childhood-onset forms exhibit disease-specific skeletal muscle pathology, which shows fibers occupied by huge vacuoles that contain basophilic amorphous materials. However, diagnosis of the adult-onset form is sometimes challenging due to clinical similarities to muscular dystrophy and the paucity of typical vacuolated myofibers. We diagnosed 37 patients with Pompe disease including 11 infantile, 16 childhood-onset, and 10 adult-onset forms in the muscle repository of the National Center of Neurology and Psychiatry (NCNP), Japan, based on a deficiency of GAA enzyme activity assayed using biopsied muscles, as previously described [2]. Among these 37 patients, two unrelated Japanese patients did not have disease-specific vacuolated muscle fibers but did have unique cytoplasmic inclusions. Here, we report the diagnostic utility of acid phosphatase (ACP)-positive globular inclusions for adult-onset Pompe disease.

* Corresponding author. Address: National Institute of Neuroscience, National Center of Neurology and Psychiatry, 4-1-1 Ogawahigashi-cho, Kodaira, Tokyo 187-8502, Japan. Tel.: +81 42 341 2711; fax: +81 42 346 1742.
E-mail address: nishino@ncnp.go.jp (I. Nishino).

0960-8966/$ - see front matter © 2011 Elsevier B.V. All rights reserved.
doi:10.1016/j.nmd.2011.11.003

2. Case report

2.1. Clinical summary

Patient 1: A 44-year-old man had been well until the age of 41 years when he started having difficulty in running. He was admitted to the hospital because of progressive muscle weakness. His parents were first cousins, but there was no family history of neuromuscular disorders. He was clinically suspected to suffer from muscular dystrophy because of slowly progressive muscle weakness and elevated creatine kinase levels of around 800 IU/L (normal, <171 IU/L). On examination, he had grade 4-muscle weakness on medical research council (MRC) scale and marked atrophy in his thighs. He did not have apparent respiratory impairment. Electromyography (EMG) showed myopathic changes with fibrillation and increased polyphasic motor unit potentials (MUPs).

Patient 2: A 62-year-old woman first noticed difficulty in climbing stairs at the age of 35 years, and needed a stick to walk at 45 years. Muscle weakness gradually worsened predominantly in her proximal limbs, and she became wheelchair-bound at 55 years. A muscle biopsy was performed at the age of 61 years. On examination, she had muscle weakness and atrophy predominantly in the proximal upper and lower limbs at the grade 3–4 on MRC scale. Serum CK level was 70 IU/L (normal, <142 IU/L). An EMG showed myopathic changes with increased polyphasic MUPs and myotonic-like repetitive discharges. She had been on non-invasive positive-pressure ventilation since the age of 62 years when the respiratory insufficiency appeared.

2.2. Skeletal muscle pathology

The skeletal muscle pathology from the vastus lateralis of patient 1 and from the biceps brachi of patient 2 showed nonspecific myopathic changes with moderate fiber size variation, mild endomysial fibrosis, and some fiber splitting (Fig. 1A). No necrotic or regenerating fibers were seen. No vacuoles containing amorphous materials were observed. Importantly, both muscles contained red–purple globular inclusions on modified Gomori-trichrome (mGT) stain (Fig. 1A and B). The average percentages of fibers with globular inclusions in the whole mGT-stained section were 0.5% in patient 1 and 2% in patient 2. These inclusions were invariably highlighted by ACP stain but not stained by periodic acid Schiff (PAS) (Fig. 1C). Inclusions were stained only faintly on menadione-linked α-glycerophosphate dehydrogenase (MAG) without substrate (Fig. 3A). Fibers with ACP-positive globular inclusions were also found in 15 of 16 childhood-onset and seven of eight adult-onset patients with disease-specific pathology in varying proportions (0.1–10%). The rate of fibers with inclusions was not significantly different between the childhood-onset and adult-onset forms. Fibers carrying inclusions did not have typical vacuoles with amorphous materials inside. In the infantile cases, more than 90% of the fibers were vacuolated, whereas non-vacuolated fibers with inclusions were hardly recognizable.

Double immunostaining was performed using primary antibodies against a lysosomal marker, lysosomal associated membrane protein-2 (LAMP-2; Developmental Studies Hybridoma Bank (DSHB), Iowa City, IA, USA) and an autophagosomal marker, microtubule-associated protein 1 light chain 3 (LC3; Novus Biologicals, Littleton, CO, USA). In fibers with ACP-positive inclusions, immunoreactivity for LAMP-2 and LC3 were accumulated focally in inclusions and surrounding area (Fig. 1D). We also examined another samples from adult-onset patients with typical vacuoles. Fibers with typical vacuoles were entirely positive for LAMP-2 and LC3 (data not shown).

On PAS staining, performed on epon-embedded sections (Epon-PAS) to detect glycogen more sensitively, PAS was negative in globular inclusions but positive in the surrounding area (Fig. 1E).

Electron micrography was performed as previously described using a Tecnai spirit transmission electron microscope (FEI, Hillsboro, OR, USA) [3]. The inclusions consisted of homogeneous electron-dense globules surrounded by increased glycogen particles and autophagic vacuoles (Fig. 1F). The globules contained neither dotted glycogen particles nor a filamentous structure.

2.3. GAA enzymatic analysis and genetic analysis

Presence of globular inclusions led us to suspect Pompe disease, and GAA enzymatic activity analyses revealed 7.5% of normal control activity in patient 1 and 12.3% in patient 2.

Genomic DNA was extracted from peripheral lymphocytes or biopsied muscle using a standard protocol for mutational analysis of *GAA*. All exons and their flanking intronic regions of *GAA* were amplified by PCR and directly sequenced with an ABI PRISM 3100 Automated Sequencer (Applied Biosystems, Foster City, CA, USA). Both patients carried the homozygous *GAA* mutation at the last codon of exon 2 (c. 546G > T). RT-PCR and direct sequencing were performed using RNA extracted from biopsied muscles. This novel mutation causes aberrant splicing by skipping exon 2 (Fig. 2). This homozygous c. 546G > T mutation was also found in another patient with the adult-onset form, whose muscle pathology showed typical skeletal muscle pathology with vacuolated fibers.

3. Discussion

ACP-positive globular inclusions were a good diagnostic marker for the two patients with adult-onset Pompe disease lacking typical vacuolated fibers. Among 12,103 muscle biopsies in the NCNP repository from 1979 to 2010, ACP-positive globular inclusions were not reported, except for Pompe disease.

The globular inclusions are most likely the same as "reducing body-like globular inclusions in late-onset Pompe disease" reported by Sharma et al., as the pathological features are

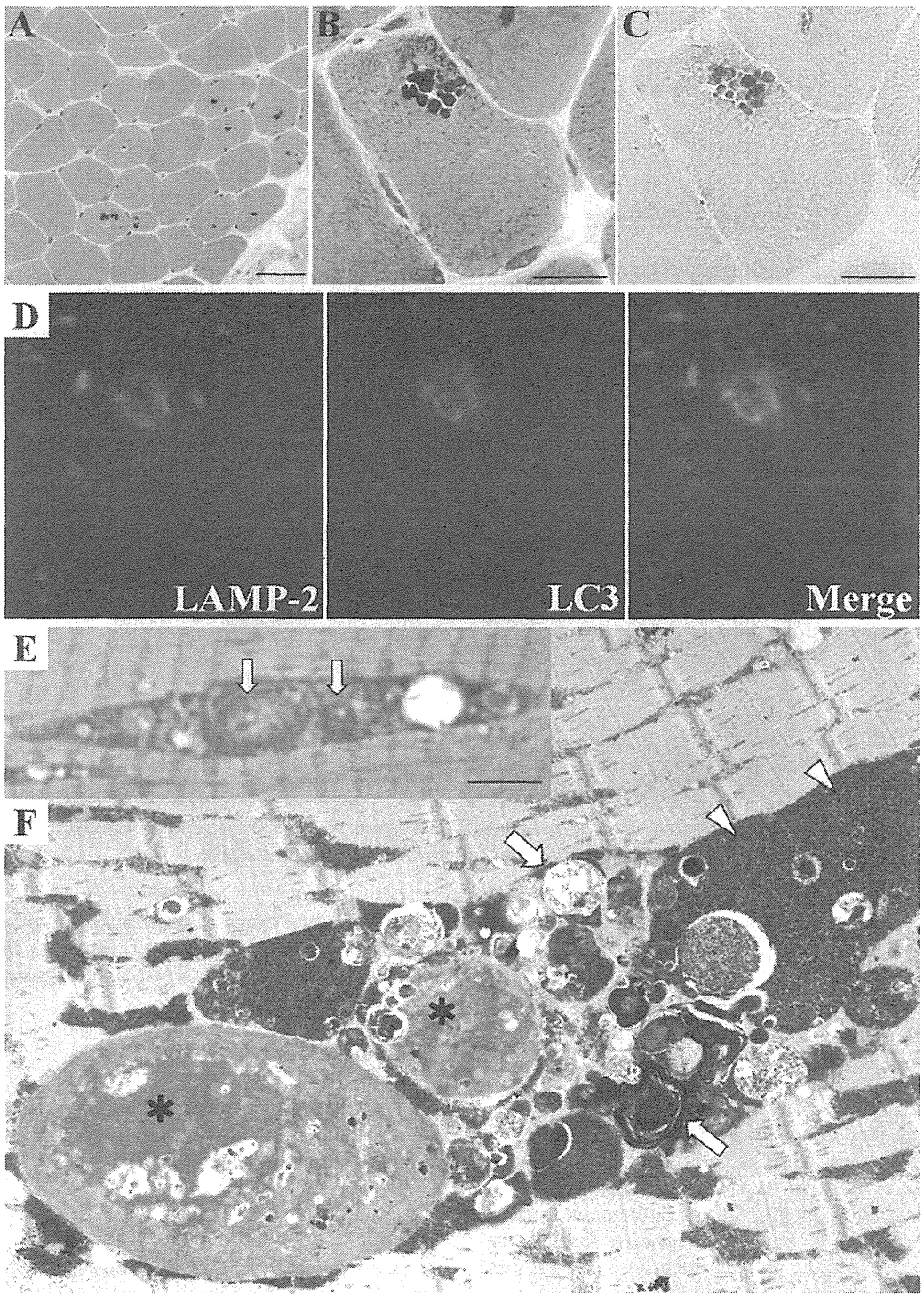

Fig. 1. Acid phosphatase-positive globular inclusions in patient 2. (A and B) Biopsied skeletal muscle showed nonspecific myopathic changes with scattered red–purple colored globular inclusions on modified Gomori-trichrome stain. (C) The inclusions have intense activity on acid phosphatase stain. Bar = 20 μm. (D) Double immunostaining for LAMP-2 (green) and LC3 (red) demonstrates colocalization of positive immunoreactions in the inclusions and surrounding area (B–D; serial sections). (E) On epon-embedded section, periodic acid Schiff stain is negative in inclusions (arrows). Bar = 5 μm. (F) On electron microscopy, globular inclusions (asterisks) lack Z-line structure, which differs from cytoplasmic bodies. Autophagic vacuoles (arrows) and glycogen particles (arrow heads) are seen in the vicinity of globular inclusions (12000×).

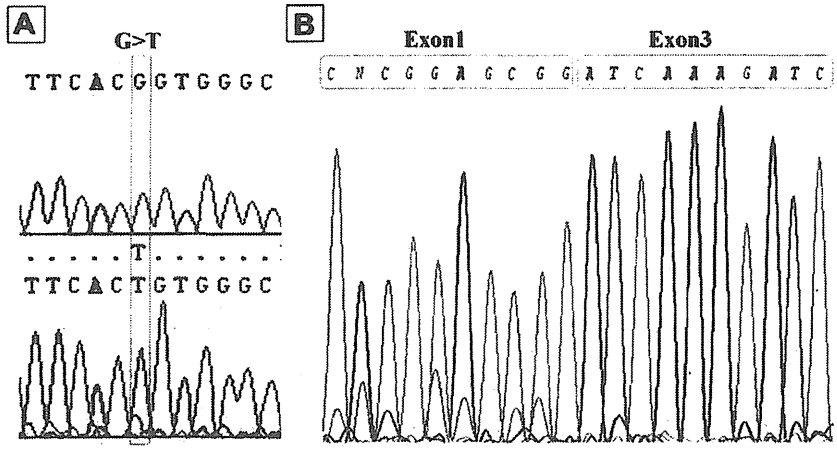

Fig. 2. Mutational analysis of *GAA*. Both patient have a homozygous c. 546G > T mutation at the last codon of exon2 (A upper: control, lower: patient), which creates mRNA with skipping exon 2 (B).

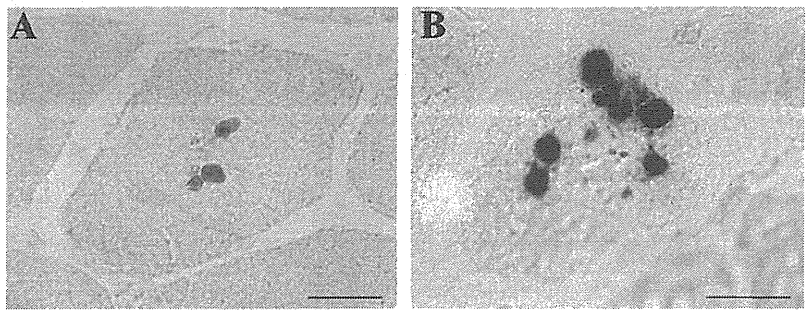

Fig. 3. Inclusions on menadione-linked α-glycerophosphate dehydrogenase (MAG) without substrate. Globular inclusions in Pompe disease (A) are only faintly stained comparing reducing bodies in reducing body myopathy with *FHL1* mutation (B). Bar = 20 μm.

rather similar [4]. However, globular inclusions showed much fainter staining on MAG without substrate than genuine reducing bodies seen in reducing body myopathy with *FHL1* mutations (Fig. 3). More importantly, ACP positivity has not been clearly described previously.

These globular inclusions are reminiscent of cytoplasmic bodies, which are nonspecific findings reflecting degeneration of the Z-disk in various neuromuscular diseases, particularly myofibrillar myopathies. However, the nature of the globular inclusions differs essentially from cytoplasmic bodies because of positive ACP staining and the lack of associated Z-disk components. Although it remains unclear how the ACP-positive globular inclusions are formed, the absence of glycogens in the globular inclusions suggest that they differ from glycogen accumulations in lysosomes. Fibers with typical vacuoles were diffusely positive for both lysosomal and autophagosomal markers as shown previously [5,6]. On the other hand, immunoreactivities of these markers accumulated more focally in fibers with inclusions. Further study should be needed to clarify what causes these pathological differences.

In conclusion, ACP-positive globular inclusions may be a hallmark of Pompe disease and a useful diagnostic marker for adult-onset Pompe disease lacking typical vacuolated fibers. Since enzyme replacement therapy is effective, albeit not fully, in adult-onset patients, early diagnosis is necessary for a better prognosis.

Ethical approval

All clinical materials used in this study were obtained for diagnostic purposes with written informed consent approved by the Ethical Committee of NCNP.

Acknowledgements

We are grateful to Satomi Mitsuhashi, Kaoru Tatezawa, Yuriko Kure, Mieko Ohnishi, and Kanako Goto (NCNP) for their technical assistance, to May Christine V. Malicdan (National Human Genome Research Institute, National Institutes of Health) for reviewing the manuscript. This study was supported by: a Grant-in-Aid for Scientific Research from Japan Society for the Promotion of Science; Research on Psychiatric and Neurological Diseases and Mental Health, Research on Measures for Intractable Diseases, Health Labor Sciences Research

Grant for Nervous and Mental Disorders (20B-12, 20B-13) from the Ministry of Health, Labor, and Welfare, and Intramural Research Grant (23-4, 23-5) for Neurological and Psychiatric Disorders from NCNP.

References

[1] Hers HG. Alpha-glucosidase deficiency in generalized glycogen storage disease (Pompe's disease). Biochem J 1963;86:11–6.
[2] Shanske S, Dimauro S. Late-onset acid maltase deficiency. Biochemical studies of leukocytes. J Neurol Sci 1981;50:57–62.
[3] Park YE, Hayashi YK, Goto K, et al. Nuclear changes in skeletal muscle extend to satellite cells in autosomal dominant Emery-Dreifuss muscular dystrophy/limb-girdle muscular dystrophy 1B. Neuromuscul Disord 2009;19:29–36.
[4] Sharma MC, Schultze C, von Moers A, et al. Delayed or late-onset type II glycogenosis with globular inclusions. Acta Neuropathol 2005;110:151–7.
[5] Raben N, Ralston E, Chien YH, et al. Differences in the predominance of lysosomal and autophagic pathologies between infants and adults with Pompe disease: implications for therapy. Mol Genet Metab 2010;101:324–31.
[6] Schoser BGH, Müller-Höcker J, Horvath R, et al. Adult-onset glycogen storage disease type 2: clinico-pathological phenotype revisited. Neuropathol Appl Neurobiol 2007;33:544–59.

Available online at www.sciencedirect.com

SciVerse ScienceDirect

Neuromuscular Disorders 22 (2012) 162–165

www.elsevier.com/locate/nmd

Case report

Muscle glycogen storage disease 0 presenting recurrent syncope with weakness and myalgia

Sayuri Sukigara [a], Wen-Chen Liang [b,c], Hirofumi Komaki [a], Tokiko Fukuda [d], Takeshi Miyamoto [e], Takashi Saito [a], Yoshiaki Saito [a], Eiji Nakagawa [a], Kenji Sugai [a], Yukiko K. Hayashi [b], Hideo Sugie [d], Masayuki Sasaki [a], Ichizo Nishino [b,*]

[a] *Department of Child Neurology, National Center Hospital, National Center of Neurology and Psychiatry (NCNP), Kodaira, Tokyo, Japan*
[b] *Department of Neuromuscular Research, National Institute of Neuroscience, NCNP, Kodaira, Tokyo, Japan*
[c] *Department of Pediatrics, Kaohsiung Medical Univeristy Hospital, Kaohsiung Medical University, Kaohsiung, Taiwan*
[d] *Department of Pediatrics, Jichi Medical University and Jichi Chidren's Medical Center, Shimotsuke, Tochigi, Japan*
[e] *Department of Pediatrics, Kosai Municipal Hospital, Kosai, Shizuoka, Japan*

Received 22 March 2011; received in revised form 17 June 2011; accepted 22 August 2011

Abstract

Muscle glycogen storage disease 0 (GSD0) is caused by glycogen depletion in skeletal and cardiac muscles due to deficiency of glycogen synthase 1 (GYS1), which is encoded by the *GYS1* gene. Only two families with this disease have been identified. We report a new muscle GSD0 patient, a Japanese girl, who had been suffering from recurrent attacks of exertional syncope accompanied by muscle weakness and pain since age 5 years until she died of cardiac arrest at age 12. Muscle biopsy at age 11 years showed glycogen depletion in all muscle fibers. Her loss of consciousness was gradual and lasted for hours, suggesting that the syncope may not be simply caused by cardiac event but probably also contributed by metabolic distress.

Keywords: Glycogen storage disease; Glycogen synthase; Glycogen; Syncope; Sudden death

1. Introduction

Glycogen is a high molecular mass polysaccharide that serves as a repository of glucose for use in times of metabolic need. It is stored in liver, cardiac and skeletal muscles, and broken down to glucose to produce ATP as energy as needed. For the synthesis of glycogen, at least two proteins, glycogenin (GYG) and glycogen synthase (GYS), are known to be essential. GYG is involved in the initiation reactions of glycogen synthesis: the covalent attachment of a glucose residue to GYG is followed by elongation to form an oligosaccharide chain [1]. GYS catalyzes the addition of glucose monomers to the growing glycogen molecule through the formation of alpha-1,4-glycoside linkages [2].

Defect in either GYG or GYS can cause glycogen depletion. Recently, muscle glycogen deficiency due to a mutation in a gene encoding muscle GYG, *GYG1*, was reported [3] and named as glycogen storage disease type XV. In contrast, glycogen depletion caused by the *GYS* gene mutation is called glycogen storage disease type 0 (GSD0). GSD0 was first reported in 1990 in patients with type 2 diabetes who had a defect in glycogen synthesis in liver, which was caused by a defect in liver GYS, GYS2, and the disease was named as liver GSD0 (or also called GSD0a) [4,5].

The disease of muscle GYS, GYS1, was first described in 2007 in three siblings and named muscle GSD0, which is

* Corresponding author. Address: Department of Neuromuscular Research, National Institute of Neuroscience, NCNP, 4-1-1, Ogawahigashi-cho, Kodaira, Tokyo 187 8551, Japan. Tel.: +81 42 3412711; fax: +81 42 3427521.
E-mail address: nishino@ncnp.go.jp (I. Nishino).

0960-8966/$ - see front matter © 2011 Elsevier B.V. All rights reserved.
doi:10.1016/j.nmd.2011.08.008

also called GSD0b [6]. One of the patients initially manifested exercise intolerance, epilepsy and long QT syndrome since the age of 4 years, then died of sudden cardiac arrest after exertion when he was 10.5-year-old. The other two siblings were then genetically confirmed as muscle GSD0 with mutations in *GYS1* and cardiac involvement was also found in both. The second muscle GSD0 family was reported in 2009 [7]. The 8-year-old boy had been healthy before collapsing during a bout of exercise, resulting in death. Post-mortem examinations and studies verified the diagnosis of muscle GSD0. He had a female sibling who died at 6 days of age of undetermined cause. Here we report the first muscle GSD0 patient in Asia with some distinct clinical manifestations from other reported cases.

2. Case report

An 11-year-old Japanese girl with repeated episodes of post-exercise loss of consciousness, weakness, and myalgia since age 5 years, was admitted to the hospital. She was the first child of unrelated healthy parents. She was born uneventfully and was normal in psychomotor development. At age 2 years, she developed the first episode of generalized tonic-clonic seizure while she was sleeping. At age 4 years, she had the second episode of generalized tonic-clonic seizure when she was under general anesthesia for tonsillectomy, whose cause was thought to be hypoglycemia due to prolonged fasting. In both episodes, seizure was followed by strong limb pain. At age 5 years, she suffered from the first episode of syncope while climbing up stairs. She recovered after a few hours. One year later, she had the second syncopal attack after running 50 m, which was accompanied by subsequent limb muscle weakness and myalgia. Since then, similar episodes were repeated several times a year. For each bout, she first developed leg muscle weakness immediately after exercise, making her squat down, and gradually lost the consciousness. She recovered her consciousness after a few hours but always experienced strong myalgia in legs which lasted for several hours. Blood glucose level was not decreased during these attacks.

On admission, general physical examination revealed no abnormal finding. On neurological examination, she had mild proximal dominant muscle weakness and mildly limited dorsiflexion of both ankle joints. T1-weighted images of skeletal muscle MRI showed high signal intensities in gluteal and flexor muscles of the thigh, which were assessed to be fatty degeneration (Fig. 1). Systemic investigations including electrocardiography, echocardiography, stress cardiac catheterization, stress myocardial scintigraphy, brain imaging, electroencephalography, and screening tests for metabolic diseases revealed no abnormality except for a mild ischemic finding on exercise electrocardiography. Ischemic and non-ischemic forearm exercise tests [8] showed the lack of lactate elevation, raising a possibility of glycogen storage disease. A few months later, resting electrocardiography, 24-h holter monitoring and resting echocardiography were re-evaluated and again revealed normal findings.

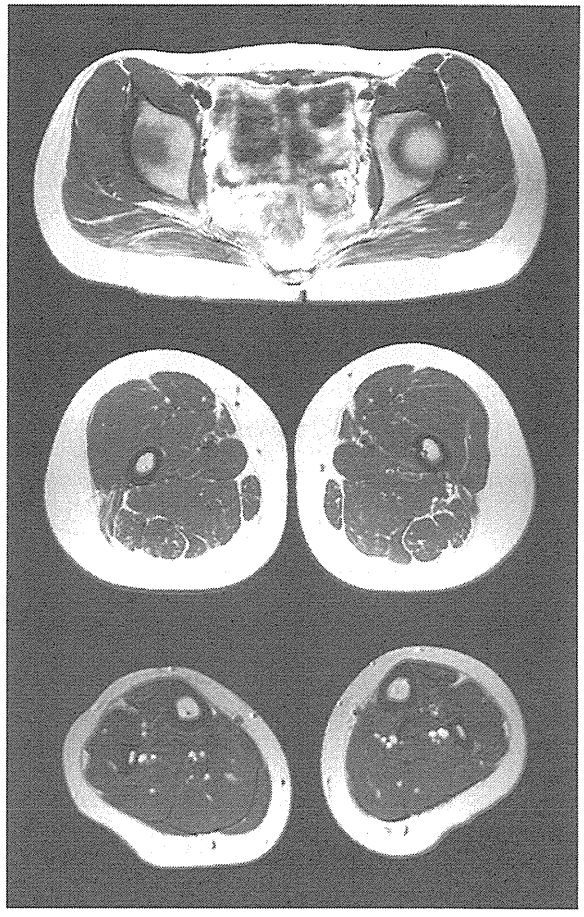

Fig. 1. Muscle MRI, T2WI, axial. It shows high intensity in gluteus maximus and biceps femoris muscles.

3. Histological analysis of skeletal muscle

Muscle biopsy was performed from biceps brachii. Serial frozen sections were stained with hematoxylin and eosin, modified Gomori trichrome, and a battery of histochemical methods. The most striking finding was depletion of glycogen in all muscle fibers but not in the interstitium on periodic acid-schiff (PAS) staining (Fig. 2A). Phosphorylase activity was also deficient in all fibers (Fig. 2B). Mitochondria especially at the periphery of muscle fibers were prominent on modified Gomori trichrome (Fig. 2D). ATPase staining revealed type 2 fiber atrophy. Electron microscopic analysis showed mitochondrial proliferation at the periphery of muscle fibers with no notable intramitochondrial inclusions (Fig. 2E).

4. Biochemical and molecular analysis

Both the activity of GYS1 and the amount of glycogen in the skeletal muscle were markedly reduced (Table 1). On western blotting, GYS1 in the patient's skeletal muscle was undetectable (Fig. 2F). The *GYS1* gene sequence analysis revealed compound heterozygous mutation of

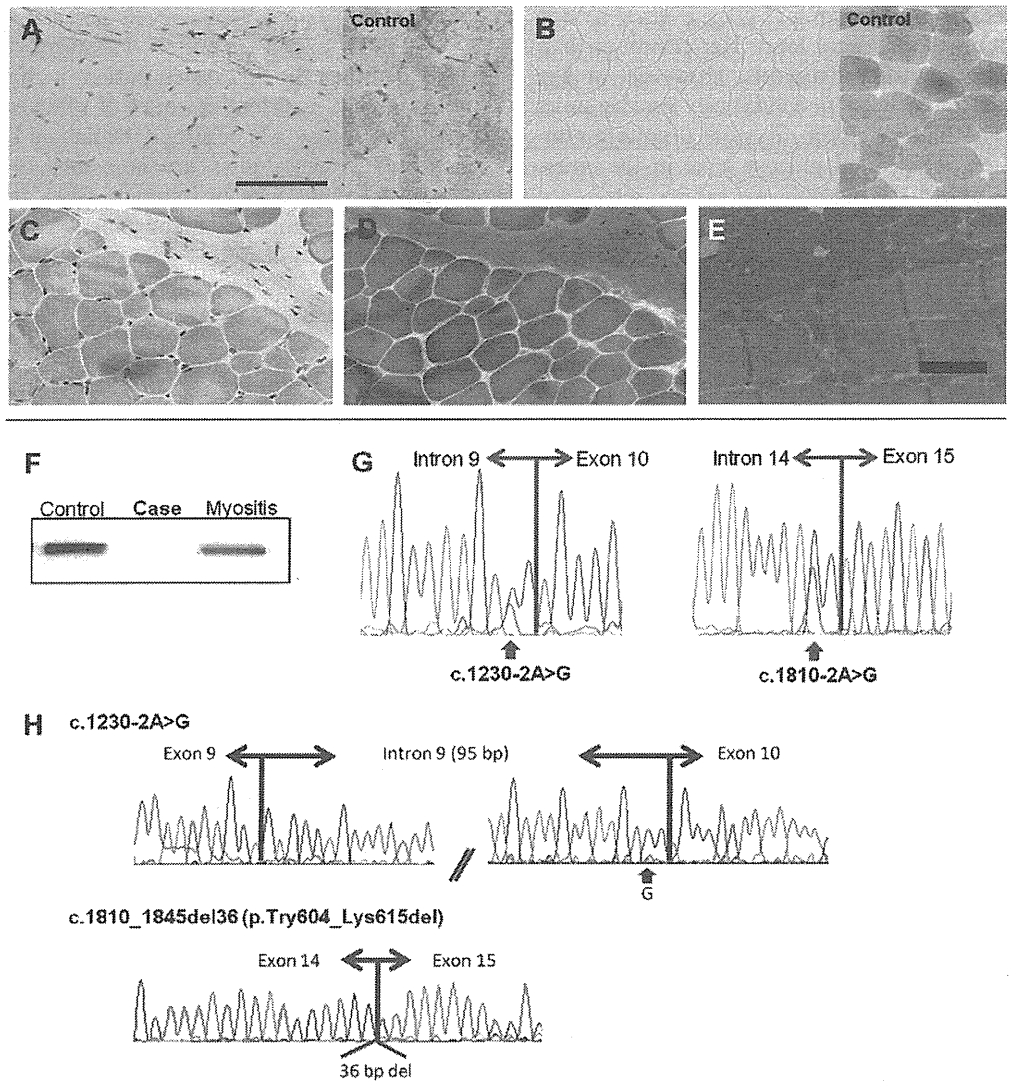

Fig. 2. Histological, genetic and protein analyses. Periodic acid-schiff (PAS) staining shows marked depletion of glycogen in muscle fibers but not in the interstitium (A). Phosphorylase activity is also deficient in all fibers (B). Hematoxylin and eosin staining shows mild fiber size variation (C). On modified Gomori trichrome, mitochondria are prominent especially at the margin of each muscle fiber (D). On electron microscopy (EM), mitochondria are increased in number at the periphery of muscle fibers (E). Bars represent 100 μm for histochemistry and 7 μm for EM. On western blotting using anti-GYS1 antibody (Abcam), GYS1 protein is absent in skeletal muscle from the patient (F). Sequence analysis for the *GYS1* gene reveals a compound heterozygous mutation of c.1230-2A > G and c.1810-2A > G (G). cDNA analysis showed insertion of intron 9 between exon 9 and 10 and 36-bp deletion from the beginning of exon 15 (H).

Table 1
Analyses of enzymatic activity and glycogen content. The activity of GYS and glycogen content in skeletal muscle were markedly reduced.

	Glycogen synthase (mol/min/mg)	UDPG-pyrophosphorylase (nmol/min/mg)	Glycogen contents (% of wet weight)
Patient	*0.9*	30.5	*0.03*
Control	42.0 ± 11.2	31.2 ± 3.5	0.94 ± 0.55

Italicized values: lower than control range.

c.1230-2A > G in intron 9 and c.1810-2A > G in intron 14 (Fig. 2G). cDNA analysis confirmed the insertion of the full-length intron 9 between exons 9 and 10 and a 36-bp deletion in the beginning of exon 15 (Fig. 2H).

5. Clinical course after diagnosis

Upon the diagnosis of GSD0, exercise was strictly limited to avoid syncope resulted from glucose depletion. In

addition, oral intake of cornstarch (2 g/kg, every 6 h) was started to maintain blood sugar level. Her condition had been stable for 1 year after diagnosis. However, at age 12 years, she was found lying unconsciously on the stairs at her school. She had persistent asystole despite ambulance resuscitation. The blood glucose level in the emergency room was above 100 mg/dl.

6. Discussion

We identified the first Asian patient with muscle GSD0, who manifested recurrent episodes of syncope with subsequent muscle weakness and myalgia, and eventually developed cardiac arrest.

Findings in our patient seem to be similar to previous reports, but some differences indicated the possibility of another pathogenesis of the disease. Our patient repeatedly suffered from episodes of syncope. In contrast to two earlier reports, those patients never had syncope, although the last attack led to sudden death [6,7]. In support of this notion, most muscle glycogen synthase knock-out mice died soon after birth due to impaired cardiac function [8]. However, the pattern of loss of consciousness in our patient cannot be explained by simple cardiac dysfunction, as she lost her consciousness gradually after exercise and took hours to regain, which is different from typical cardiac syncope, usually showing sudden loss of consciousness and rapid recovery. Alternatively, defective glycogen synthesis in brain may be related to syncope, as GYS1 is also expressed in brain, albeit not so much as in cardiac and skeletal muscles. Another possibility may be intermittent arrhythmia. However, electrocardiogram during the episode was never obtained. Further studies are necessary to answer this question.

On muscle pathology and electron microscopy, we found profound deficiency of glycogen in all muscle fibers accompanied by mitochondrial proliferation, which is similar to previous reports. The mitochondrial proliferation may reflect a compensatory mechanism for supplying ATP to glycogen-depleted muscles. Interestingly, phosphorylase activity on histochemistry seemed deficient. This is consistent with the fact that endogenous glycogen is used as a substrate of phosphorylase on histochemistry. Previous reports described the reduced number of type 2 fibers. In our patient, type 2 fiber atrophy, but not type 2 fiber deficiency, was seen. Although type 2 fiber atrophy is a nonspecific finding, this picture might also reflect the dysfunction of glycogen-dependent muscle fibers.

7. Conclusion

We identified the first Asian patient with muscle GSD0. In our patient, recurrent episodes of syncope and eventual sudden death may not be simply explained by cardiac dysfunction. Further studies are necessary to elucidate the mechanism of syncope in muscle GSD0 and to establish appropriate guideline of management for these patients to prevent sudden death.

Acknowledgments

The authors thank Ms. Goto and Ms. Ogawa (National Center of Neurology and Psychiatry) for technical assistance in mutation analysis. This work is supported by: a Grant-in-Aid for Scientific Research from Japan Society for the Promotion of Science; Research on Psychiatric and Neurological Diseases and Mental Health, Research on Measures for Intractable Diseases, Health Labour Sciences Research Grant for Nervous and Mental Disorders (20B-12, 20B-13) from the Ministry of Health, Labor, and Welfare, and Intramural Research Grant (23-4, 23-5, 23-6) for Neurological and Psychiatric Disorders of NCNP.

References

[1] Viskupic E, Cao Y, Zhang W, Cheng C, DePaoli-Roach AA. Roach PJ. J Biol Chem 1992;267:25759–63.
[2] Pederson BA et al. Abnormal cardiac development in the absence of heart glycogen. Mol Cell Biol 2004;24:7179–87.
[3] Moslemi AR, Lindberg C, Nilsson J, Tajsharghi H, Andersson B, Oldfors A. Glycogenin-1 deficiency and inactivated priming of glycogen synthesis. N Eng J Med 2010;362:1203–10.
[4] Shulman GI, Rothman DI, Jue T, Stein P, DeFronzo PA, Shulman RG. Quantitation of muscle glycogen synthesis in normal subjects and subjects with non-insulin-dependent diabetes by 13C nuclear magnetic resonance spectroscopy. N Eng J Med 1990;322:223–8.
[5] Orho M, Bosshard NU, Buist NR, Gitzelmann R, Aynsley-Green A, Blümel P, et al. Mutations in the liver glycogen synthase gene in children with hypoglycemia due to glycogen storage disease type 0. J Clin Invest 1998;102:507–15.
[6] Kollberg G, Tulinius M, Gilljam T, Ostman-Smith I, Forsander G, Jotorp P, et al. Cardiomyopathy and exercise intolerance in muscle glycogen storage disease 0. N Engl J Med 2007;357:1507–14.
[7] Cameron JM, Levandovskiy V, MacKay N, Utgiker R, Ackerley C, Chiasson D, et al. Identification of a novel mutation in *GYS1* (muscle-specific glycogen synthase) resulting in sudden cardiac death, that is diagnosable from skin fibroblasts. Mol Genet Metab 2009;98:378–82.
[8] Pederson BA, Cope CR, Schroeder JM, Smith NW, Irimia JM, Thurberg BL, et al. Exercise capacity of mice genetically lacking muscle glycogen synthase: in mice, muscle glycogen is not essential for exercise. J Biol Chem 2005;280:17260–5.

RESEARCH ARTICLE

Human Mutation

OFFICIAL JOURNAL
HGVS
HUMAN GENOME VARIATION SOCIETY
www.hgvs.org

Molecular Basis of Two-Exon Skipping (Exons 12 and 13) by c.1248+5g>a in *OXCT1* Gene: Study on Intermediates of *OXCT1* Transcripts in Fibroblasts

Tomohiro Hori,[1] Toshiyuki Fukao,[1,2]* Keiko Murase,[1] Naomi Sakaguchi,[1] Cary O. Harding,[3] and Naomi Kondo[1]

[1]*Department of Pediatrics, Graduate School of Medicine, Gifu University, Gifu, Gifu, Japan;* [2]*Medical Information Sciences Division, United Graduate School of Drug Discovery and Medical Information Sciences, Gifu University, Gifu, Gifu, Japan;* [3]*Department of Molecular and Medical Genetics, Oregon Health & Science University, Portland, Oregon*

Communicated by Peter H. Byers

Received 2 April 2012; accepted revised manuscript 30 November 2012.
Published online 21 December 2012 in Wiley Online Library (www.wiley.com/humanmutation). DOI: 10.1002/humu.22258

ABSTRACT: The molecular basis of simultaneous two-exon skipping induced by a splice-site mutation has yet to be completely explained. The splice donor site mutation c.1248+5g>a (IVS13) of the *OXCT1* gene resulted predominantly in skipping of exons 12 and 13 in fibroblasts from a patient (GS23) with succinyl-CoA:3-ketoacid CoA transferase (SCOT) deficiency. We compared heteronuclear RNA (hnRNA) intermediates between controls' and GS23's fibroblasts. Our strategy was to use RT-PCR of hnRNA to detect the presence or absence of spliced exon clusters in RNA intermediates (SECRIs) comprising sequential exons. Our initial hypothesis was that a SECRI comprising exons 12 and 13 was formed first followed by skipping of this SECRI in GS23 cells. However, such a pathway was revealed to be not a major one. Hence, we compared the intron removal of SCOT transcript between controls and GS23. In controls, intron 11 was the last intron to be spliced and the removal of intron 12 was also rather slow and occurred after the removal of intron 13 in a major pathway. However, the mutation in GS23 cells resulted in retention of intron 13, thus causing the retention of introns 12 and 11. This "splicing paralysis" may be solved by skipping the whole intron 11–exon 12–intron 12–exon 13–mutated intron 13, resulting in skipping of exons 12 and 13.
Hum Mutat 34:473–480, 2013. © 2012 Wiley Periodicals, Inc.

KEY WORDS: two-exon skipping; splicing order; splice site; heteronuclear RNA; SCOT; succinyl-CoA:3-ketoacid CoA transferase

Introduction

Transcription of mRNA precursors by RNA polymerase II and their splicing by the spliceosome are essential steps in gene expression. Moreover, splicing is cotranscriptional [Maniatis and Reed, 2002]. Splicing is thus ordered but not processive [Gudas et al. 1990; Kessler et al. 1993; Lang and Spritz 1987].

Most introns have conserved 5′ (donor) and 3′ (acceptor) sequences that flank the exons, a short polypyrimidine tract adjacent to the acceptor site, and a branch point sequence 18–40 nucleotides upstream from the acceptor dinucleotide [Berget, 1995; Hawkins, 1988]. Mutations in these sites can lead to exon skipping, short deletions, or insertions in the mature mRNA. It is difficult to predict the effects of splice-site mutations and understanding requires analysis of the various mRNA spliced products in cells that express the target gene. Mutations affecting splicing are a major fraction of disease-causing mutations in humans. The mechanisms whereby gene mutations result in aberrant splicing are mostly apparent from current exon-definition models of splicing [reviewed by Berget, 1995].

There are some examples where a single nucleotide substitution at such splice junctions causes the skipping of two exons [Fang et al., 2001; Haire et al., 1997; Hayashida et al., 1994; Schneider et al., 1993; Takahara et al., 2002]. The mechanisms for multiple skipping are not apparent from current exon- and intron-definition models of splicing [Takahara et al., 2002] and not well understood. The unusual occurrence of a two-exon skip may be explained by the order of intron removal in this region such that an intron is removed rapidly, in most transcripts, with respect to adjacent two introns, so that a large exon-like structure can then be skipped [Takahara et al., 2002]. In this article, we designate such an exon-like structure as a spliced exon cluster in RNA intermediates (SECRIs). Splicing order, therefore, may be an important factor in the understanding of outcomes of splice-site mutations and that multiple products are derived from different splicing pathways. Kessler et al. (1993) reported a method to determine the order of intron removal using RT-PCR, followed by several reports that determined the order of intron removal using this method [Attanasio et al., 2003; Schwarze et al., 1999; Takahara et al., 2002].

Succinyl-CoA:3-ketoacid CoA transferase (SCOT, gene symbol *OXCT1*, EC 2.8.3.5, MIM #601424), a mitochondrial homodimer essential for ketone body utilization, catalyzes the activation of acetoacetate to acetoacetyl-CoA in extrahepatic tissues [Mitchell and Fukao, 2001]. SCOT deficiency (MIM #245050), clinically characterized by episodes of severe ketoacidosis, is an autosomal recessive inborn error of metabolism, first described in 1972 [Tildon and Cornblath, 1972]. Since the first description of SCOT deficiency, fewer than 30 affected probands have been reported including personal communications [Baric et al., 2001; Berry et al., 2001; Cornblath et al., 1971; Fukao et al., 1996, 2000, 2004, 2006, 2007, 2010,

Additional Supporting Information may be found in the online version of this article.

*Correspondence to: Toshiyuki Fukao, Department of Pediatrics, Graduate School of Medicine, Gifu University, 1-1 Yanagido, Gifu, Gifu 501-1194, Japan. E-mail: toshigif@umin.net

Contract grant sponsors: Ministry of Health, Labor and Welfare of Japan; Ministry of Education, Culture, Sports, Science and Technology of Japan.

2011; Kassovska-Bratinova et al., 1996; Longo et al., 2004; Merron and Akhtar, 2009; Niezen-Koning et al., 1997; Perez-Cerda et al., 1992; Pretorius et al., 1996; Rolland et al., 1998; Sakazaki et al., 1995; Snyderman et al., 1998; Song et al., 1998; Tildon and Cornblath, 1972; Yamada et al., 2007].

We describe herein the molecular basis of SCOT deficiency in a 7-month-old boy (GS23). We detected a homozygous gene mutation, c.1248+5g>a, and the simultaneous skipping of exons 12 and 13. We compared splicing order in GS23's fibroblasts with that of control cells, to understand the mechanism of two-exon skipping in GS23 cells.

Materials and Methods

Patients

The patient (GS23) was a male infant born to nonconsanguineous parents of Mexican ancestry. He suffered recurrent ketoacidotic episodes in association with intercurrent infection beginning at the age of 7 months. He was suspected to have SCOT deficiency because he had permanent ketosis. The diagnosis was confirmed by enzyme assay. This study was approved by the Ethical Committee of Gifu University School of Medicine. The parent's DNAs were not available for this study.

Fibroblasts and Enzyme Assay

Fibroblasts from GS23 and controls were cultured in Eagle's minimal essential medium containing 10% fetal calf serum (FCS). A SCOT assay was performed as described by Williamson et al. (1971), with modifications [Song et al., 1997]. Briefly, the assay mixture contained 30 μM acetoacetyl-CoA and 50 mM sodium succinate in 50 mM Tris–HCl (pH 8.5), 10 mM MgCl2, and 4 mM iodoacetamide, and SCOT activity was measured spectrophotometrically as a decrease of acetoacetyl-CoA absorption at 303 nm.

Immunoblot Analysis

Immunoblot analysis was performed as described by Fukao et al. (1997), using a mixture of antihuman SCOT antisera and antihuman mitochondrial acetoacetyl-CoA thiolase antisera as the first antibody and 30 μg of fibroblast protein extract.

Mutation Screening at Genomic Level

Genomic DNA was purified using Sepa Gene kits (EIDIA, Tokyo, Japan) from GS23's fibroblasts. Mutation analysis was performed by PCR amplification of each exon and its boundaries (at least 18 bases from the exon/intron boundaries for both directions) with a pair of intronic primers, described in Supp. Table S1, followed by direct sequencing. Genomic sequence was obtained from GenBank NM 000436.3. The identified mutation was submitted to the Leiden Open Variation Database (www.lovd.nl/OXCT1).

Nonsense-Mediated mRNA Decay Inhibition

To determine whether any observed reduction of the transcript was due to nonsense-mediated mRNA decay (NMD) [Maquat, 2005], we inhibited NMD by fibroblasts with cycloheximide (CHX) (Sigma, St. Louis, MO), a general protein translation inhibitor. Fibroblasts were left untreated or cultured in the presence of 200 μg/ml CHX for 5 hr before RNA extraction. This analysis was performed as described by Hernan et al. (2011).

cDNA Analysis

Total RNA was isolated from fibroblasts using ISOGEN kits (Nippon Gene, Tokyo, Japan). Total RNA (5 μg) was reverse transcribed in 20 μl of 50 mM Tris–HCl pH 7.5, 75 mM KCl, 3 mM $MgCl_2$, 10 mM dithiothretiol, 0.5 mM dNTPs, 200 U of M-MLV reverse transcriptase (Life Tech., Rockville, MD) with a primer mixture including 5 pmol each of SCOT-specific antisense primer, SCOT 25 5′-$^{c.1646}$CAATTATGATTATTGATGTCC-3′, GAPDH-specific antisense primer, GAPDH3 5′-^{1040}GTGCTCTTGCTGGGGCTG-3′, and oligo dT primers. The above preparation was incubated at 37°C for 1 hr. One microliters of this cDNA solution served as a PCR template. The positions of the PCR primers were numbered in relation to the adenine of the initiation methionine codon, which was assigned position +1.

The full-coding sequence of SCOT cDNA was amplified (c.–4 – 1586).

Primer SCOT 42 (sense) 5′-$^{c.-4}$GAAGATGGCGGCTCTCAAA-3′

Primer SCOT 24 (antisense) 5′-$^{c.1586}$AGCCTGGTACAAATATCC ATA-3′

To evaluate the amount of total mRNA products, GAPDH cDNA was also amplified with the following sets of primers:

GAPDH1 (sense) 5′-$^{c.4}$GGGAAGGTGAAGGTC-3′

GAPDH2 (antisense) 5′-^{c1015}AGGGGTCTTACTCCTTGGAG-3′

These cDNA sequences were obtained from GenBank accession number NM 002046.4 for GAPDH and NM 000436.3 for SCOT.

After 30 PCR cycles, amplified fragments were separated by electrophoresis on a 3.5% (w/v) polyacrylamide gel and a 1% (w/v) agarose gel, and extracted using a Geneclean II kit (BIO 101, Vista, CA). Sequences of amplified fragments were confirmed by direct sequencing.

Isolation of Nuclear RNA

Fibroblasts were grown to near confluence in 80 cm^2 flasks in DMEM with 10% FCS. The incubation was terminated by repeated rinsing with ice-cold 1× PBS to inhibit nuclear mRNA export. Nuclear and cytoplasmic fractions were separated by incubating the scraped cell pellets in a Nonidet P-40 buffer (10 mM Tris, pH 7.4; 10 mM NaCl; 3 mM MgCl2; 0.5% Nonidet P-40) for 10 min on ice, followed by centrifugation for 5 min at 1,450 ×*g*, 4°C. The supernatant contained the cytoplasmic components. The nuclear pellet was stirred by pipetting 10 times, washed in the Nonidet P-40 buffer, and centrifuged for 5 min under the same conditions as described above. The supernatant was discarded, and the pellet was used as the nuclear fraction. Nuclear RNA was isolated from the nuclear fraction using ISOGEN kits (Nippon Gene). Nuclear RNA (10 μg) was incubated in 50 μl of 1 U deoxyribonuclease (RT Grade; Nippon Gene) at 37°C for 5 min, then a 5-μl stop solution was added and it was inactivated at 70°C for 10 min.

Analysis of SECRIs by RT-PCR

The isolated nuclear RNA contains a mixture of various stages of splicing intermediates. To investigate the order of intron removal or splicing order, we analyzed the presence or absence of various SECRIs by RT-PCR. Our strategy was to first identify, using specific primer pairs, all possible SECRIs of two adjacent exons (such

as exons 2–3 fusion), then to search for SECRIs comprising three sequential exons (such as exons 1–2–3 fusion), four sequential exons , and so on. For example, if intron 12 is spliced out before the removal of introns 11 and 13, a SECRI comprising exons 12 and 13 is predicted to be amplified by a sense primer in intron 11 and an antisense primer in intron 13.

We designed PCR primers as shown in Supp. Table S1. Sense primers, ex1F to in16F, were used for amplification of exon 1 to exon 17, respectively. Antisense primers, in1R to ex17R, were for amplification of exon 1 to exon 17, respectively. To initiate cDNA synthesis from nuclear RNA, we employed additional SCOT-specific antisense primers, labeled in2R′ to ex17R′, that were located downstream from in2R to ex17R, respectively. Three separate cDNA synthesis reactions were carried out using mixtures of either in2R′, in3R′, in4R′, in5R′, and in6R′ primers, of in7R′, in8R′, in9R′, in10R′, and in11R′ primers, or of in12R′, in13R′, in14R′ in15R′, in16R′, and ex17R′ primers. The cDNA products then served as templates for PCR detection of various SECRIs using in2R, in3R, in4R, in5R, and in6R antisense primers, in7R, in8R, in9R in10R, and in11R antisense primers, or in12R, in13R, in14R in15R, in16R, and ex17R antisense primers, respectively.

All primers listed in Supp. Table S1, except for ex1F, ex11F, ex12F, ex13F, ex13R, ex14R, ex15R, ex15R′, ex17R, and ex17R′, were complementary to intronic sequences. ex1F was placed upstream from the initiation codon on exon 1. ex17R and ex17R′ were placed downstream from the termination codon on exon 17.

Nuclear RNA (2 μg) was reverse transcribed in 20 μl of 50 mM Tris–HCl pH 7.5, 75 mM KCl, 3 mM $MgCl_2$, 10 mM dithiothretiol, 0.5 mM dNTPs, the mixture of the above antisense primers (10 pmol each) and 200 U of M-MLV reverse transcriptase (Life Tech.) at 37°C for 1 hr. One microliter of this cDNA solution served as a PCR template. Specific exons were amplified using 30 pmol each of the above sense and antisense primers for 35 PCR cycles. Each cycle consisted of 1 min of denaturation at 94°C, 2 min of annealing at 60°C, and a 1-min extension at 72°C. The amplified fragments were detected following electrophoresis on a 2% (w/v) agarose gel and ethidium bromide staining. Sequences of amplified fragments were confirmed by direct sequencing.

Analysis of Intron Removal Around Exons 11–14

Fibroblasts from a control and from the patient were grown to near confluence in six-well tissue-culture plates in DMEM with 10% FCS. The medium was then replaced by serum-free DMEM, and 5 μg/ml of Actinomycin D (Roche Diagnostics, Basel, Switzerland) was added to halt transcription. The incubation was terminated after 5, 10, 20, 40, or 60 min by adding 1 ml of ISOGEN solution. One well of each cell line was left untreated to serve as a baseline control. Total RNA using ISOGEN kit (Nippon Gene) from the different timepoints was treated with Deoxyribonuclease, as described above. cDNA synthesis reactions were carried out using a mixture of SCOT-specific antisense primers in13R′, in14R′, and ex15R′ (Supp. Table S1). To check for residual genomic DNA in the RNA preparation, one PCR reaction was done without prior reverse transcription.

Results

Enzyme Assay and Immunoblot Analysis

SCOT activity in GS23's fibroblasts (0.4 ± 0.9 nmol/min/mg protein, n = 7) was less than 10% of SCOT activity in control fibroblasts (4.5 ± 1.2 nmol/min/mg protein, n = 7), whereas acetoacetyl-CoA thiolase activity in the presence of potassium ion (9.4 ± 2.6 nmol/min/mg protein, n = 7) was similar to that of controls (8.0 ± 1.7 nmol/min/mg protein, n = 7). In immunoblot analysis, SCOT protein was not detected in GS23's fibroblasts, whereas SCOT protein was clearly detected in control fibroblasts (data not shown). These analyses thus confirmed SCOT deficiency in GS23.

Gene Mutations

Sequencing of the SCOT gene in GS23 revealed an apparent homozygosity for a G to A mutation at the fifth nucleotide of intron 13 (c.1248+5g>a) (Fig. 1A). No other mutations were detected by sequencing of all exons and the exon–intron boundaries.

cDNA Analysis

We first performed RT-PCR using total RNA with CHX-untreated fibroblasts. Amplification of the SCOT cDNA (c.–4 – 1586) from control fibroblasts produced a single fragment with the expected size of 1,590 bp (Fig. 1B, control CHX–, indicated by arrow 1). However, in GS23, there were two faint shorter fragments of approximately 1,450 bp (GS23 CHX–, indicated by arrow 2) and 1,100 bp (indicated by arrow 3). Sequence analysis of these fragments revealed that the 1,450 bp fragment (indicated by arrow 2) lacked exons 12 and 13 (Fig. 1C), whereas the 1,100 bp fragment lacked exons 8–13. Because skipping of exons 12 and 13 results in a frame-shift and skipping of exons 8–13 does not, we reperformed RT-PCR using total RNA from CHX-treated and nontreated fibroblasts to confirm that the mRNA with skipping of exons 12 and 13 is a major transcript in GS23.

When we inhibited NMD by treating fibroblasts with CHX, the cDNA with skipping of exons 12 and 13 was amplified much more abundantly than the cDNA with exons 8–13 skipping in case of GS23 (Fig. 1B, GS23 CHX+), whereas no change was observed in the case of a control (Control CHX+). On the basis of this experiment, we concluded that the major transcript in GS23 had skipping of exons 12 and 13 and was subjected to NMD. On the contrary, mRNA with skipping of exons 8–13 is in-frame, and should be a minor transcript.

We considered that the mutation at the splice donor site of intron 13 (c.1248+5g>a) caused exons 12 and 13 skipping instead of solely exon 13 skipping. We tested a hypothesis that two exons were skipped because the upstream intron 12 was rapidly removed, similar to the model proposed by Takahara et al. (2002).

Analysis of RNA Intermediates Encompassing Exons 12 and 13

To test this hypothesis, we analyzed splicing of heteronuclear RNA (hnRNA) in GS23 and control fibroblasts. As shown in Figure 2, a fragment with exon 12–intron 12–exon 13 (intron 12 retained) was detected in both controls and GS23, but a SECRI comprising exons 12 and 13 was clearly identified in only the two control fibroblasts but hardly detected in GS23 fibroblasts. Amplification of hnRNA using primers specific to exons 11 and 14 yielded no product in control fibroblasts but did detect a SECRI comprising exons 11 and 14 lacking exons 12 and 13 (Fig. 2).

These results indicate that (1) the skipping of exons 12 and 13 in GS23 may not be associated with an initial fusion of exons 12 and 13; but that (2) this splice-site mutation may alter the order of intron removal in SCOT RNA processing.

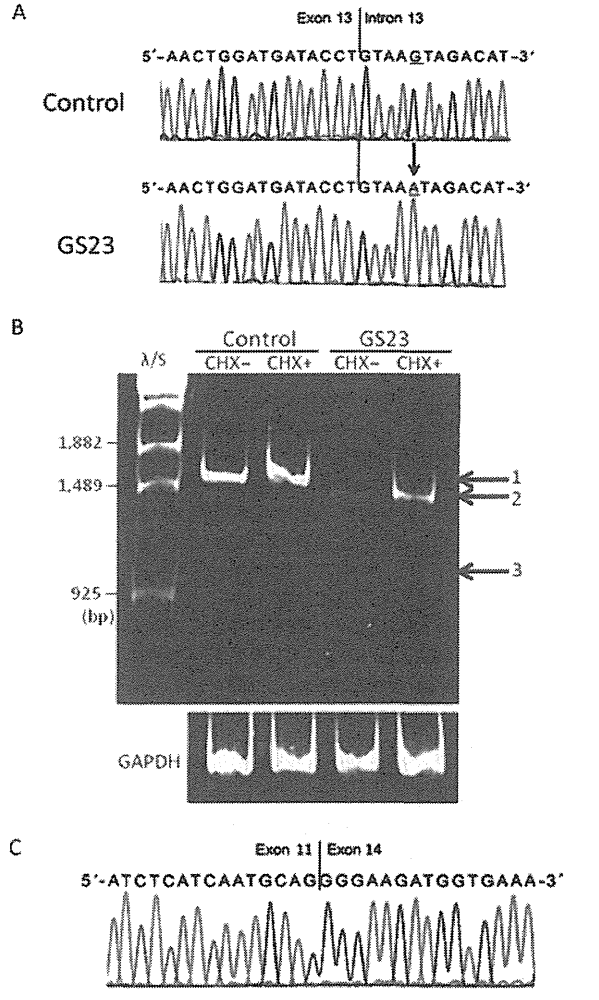

Figure 1. Genomic DNA analysis and RT-PCR analysis. **A**: An apparently homozygous point mutation from G to A was found at the fifth nucleotide of intron 13 (c.1248+5g>a) in GS23 as indicated by the arrow. **B**: RT-PCR analysis using RNAs from CHX-treated and CHX-untreated fibroblasts. SCOT cDNA (c.-4 – 1586) was amplified and electrophoresed on a 3.5% (w/v) polyacrylamide gel. In a control, a fragment with the expected size of 1,590 bp (indicated by arrow 1) was clearly detected. In GS23, a fragment with the expected size was hardly detected; however, two shorter fragments with the size of ca. 1,450 bp (indicated by arrow 2) and 1,100 bp (indicated by arrow 3) were detected. Sequence analysis of GS23's fragments revealed that the longer fragment had exons 12 and 13 skipping and the shorter one had skipping of exons 8–13. CHX: cycloheximide. **C**: Exons 12 and 13 skipping identified in GS23's cDNA.

Determination of the Last Intron to be Spliced

Our strategy was to detect hnRNA-derived cDNAs that had a solitary intron, by definition, the last intron to be spliced; such molecules would be capable of being amplified with primers from that intron and a terminal exon, as described by Kessler et al. (1993). We first detected such cDNAs using the common sense primer in exon 1 (ex1F) and a series of antisense primers in introns 2–16 (in2R–in16R) and the antisense primer in exon 17 (ex17R). In control fibroblasts (Figs. 3A and 3C), SECRIs comprising exons 1 and 2, exons 1–3, exons 1–7, exons 1–9, exons 1–11, and exons 1–17 were detected. Secondly, we used a common antisense primer on exon 17 (ex17R) and a series of sense primers from ex1F to in15F. In the two controls, SECRIs comprising exons 16 and 17, exons 15–17, exons 14–17, exons 13–17, exons 12–17, and exons 1–17 were detected. Intron 11 was the only possible solitary intron identified from both directions. These results suggested that the SECRI comprising exons 12–17 was ligated to the SECRI comprising exons 1–11 and that intron 11 removal was likely the final splicing event in controls. In addition, the amplification using a combination of in11F and ex17R produced a larger fragment including intron 12, as indicated by arrow 2 in Figure 3A, which suggested that the removal of intron 12 was also a late event. These findings are in accord with the result that no SECRI spanning exons 11–14 was amplified in controls (Fig. 2).

In the case of GS23 fibroblasts (Figs. 3B and 3D), the amplification pattern using the ex1F primer and a series of antisense primers from in2R to ex17R was similar to that of the control. However, the amplification pattern using the ex17R antisense primer and a series of sense primers from ex1F to in15F sense primers differed from that of controls. Several different pathways are possible and it is difficult to determine which pathway is the major one. Introns 7, 9, and 11 are possible last introns to be spliced in GS23 fibroblasts. In addition, a large sequence encompassing intron 11–exon 12–intorn 12–exon 13–mutated intron 13 could also be spliced out lastly.

Detection of SECRIs Flanked by Introns

We also amplified SECRIs flanked by introns. Figures 3E and 3F showed all such SECRIs detected by PCR (also see Supp. Fig. S1). In controls, SECRIs in which intron 11 was spliced out were not detected and products in which intron 12 was retained were detected (Fig. 3E). In the case of GS23, SECRIs in which mutated intron 13 was spliced out were not detected (Fig. 3F).

Comparison of Intron Removal Around Exons 11–14 Between Controls and GS23

According to the Kessler's original method [Kessler et al., 1993], several intron/exon primer pairs were used to amplify cDNA synthesized from total RNA from fibroblasts treated with Actinomycin D for different periods, although introns 11, 13, and 14 were too long to amplify intermediates including these introns (Fig. 4A).

Control fibroblasts

When we placed primers in exon 11 (ex11F) and intron 12 (in12R), no PCR products were amplified, as expected from the facts that intron 11 is too long (6,272 bp) to amplify and intron 11 is the last intron to be spliced in controls. When the primers were placed in inton 11 (in11F) and exon 13 (ex13R), the product that retained intron 12 and a SECRI in which intron 12 was spliced out were detected at 0 min. The former was no longer detectable at 60 min but the latter was still detected at 60 min. When primers were placed in exon 12 (ex12F) and intron 13 (in13R), the major product retained intron 12 and the minor product was a SECRI in which intron 12 was spliced out. Both disappeared by 60 min. When primers were placed in intron 12 (in12F) and exon 14 (ex14R), a SECRI in which intron 13 was spliced out was detected at 0 min and disappeared by 60 min. When primers were placed in exon 13 (ex13F) and intron 14 (in14R), a SECRI in which intron 13 was spliced out was clearly detected at 0 min and decreased with time. Lastly, when primers were placed in intron 13 (in13F) and exon 15

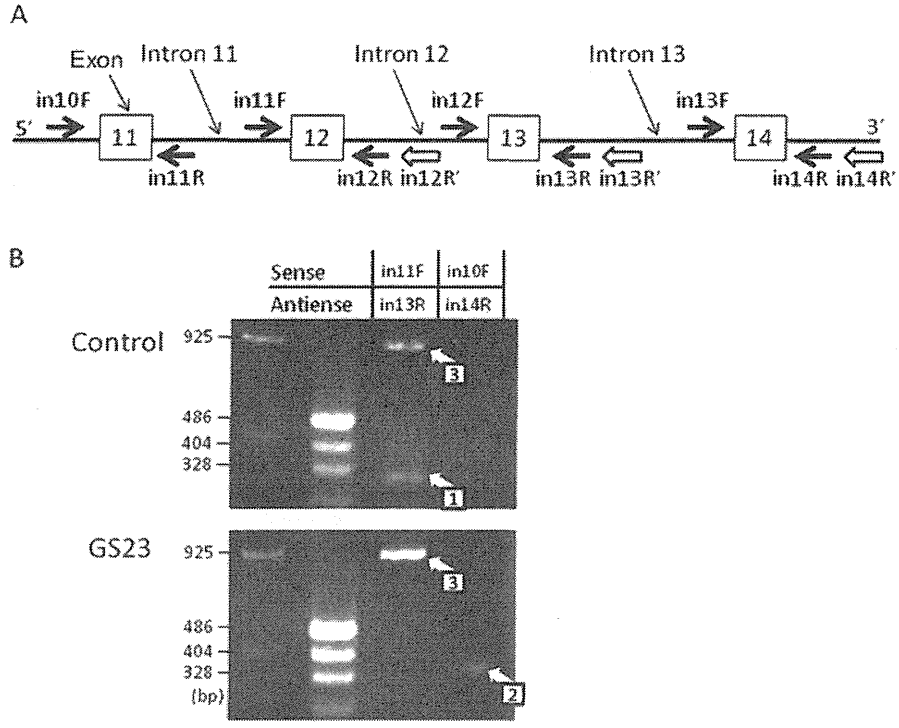

Figure 2. Analysis of RNA intermediates encompassing exons 12 and 13. **A**: Positions of the SCOT-specific primers for analysis of RNA intermediates encompassing exons 12 and 13. **B**: RT-PCR. cDNA was synthesized with isolated hnRNA using a mixture of SCOT-specific antisense primers including 12R′, 13R′, and 14R′. PCR was done using the indicated primers. A fragment with arrow 1 was a SECRI in which intron 12 was spliced out. A fragment with arrow 2 had skipping of exons 12 and 13. Fragments with arrow 3 had a retention of intron 12.

(ex15R), a SECRI in which intron 14 was spliced out was faintly detected until 40 min in the control.

GS*23 fibroblasts*

Intermediates that retained intron 12 remained with similar amounts for the full duration of the chase and no SECRIs in which intron 12 was spliced out were detected, in either primer combinations of in11F/ex13R or ex12F/in13R. The SECRIs in which intron 13 was spliced out were also not amplified in either combination of in12F/ex14R or ex13F/in14R. The SECRI in which intron 14 was spliced out was amplified with in13F and ex15R primers.

Discussion

We identified an apparently homozygous mutation c.1248+5g>a in a SCOT-deficient patient. This mutation resulted in major aberrant mRNA with skipping of exons 12 and 13. It is well known that, among donor splice-site mutations, changes at the G residue at position 1 are most commonly described, followed by mutations at position 5. Mutations at these 2 positions are thought to significantly reduce the pairing of the donor splice site with the complementary site in the small nuclear ribonucleoprotein particle U1snRNP [Kramer, 1996]. Buratti et al. (2007) summarized 346 aberrant splice donor sites that were activated by mutations in 166 human diseases. Point mutations leading to cryptic splice donor site activation were most common in the first intron nucleotide, followed by the fifth nucleotide. Substitutions at position +5 were exclusively g>a transitions. In our case, the c.1248+5g>a mutation accordingly resulted in a drastically reduced Shapiro and Senapathy score [Shapiro and Senapathy, 1987] at the authentic splice donor site of intron 13 from 79.0 (CT/gtaagt) to 64.6 (CT/gtaaat). Hence, it is predicted that c.1248+5g>a should cause aberrant splicing such as exon 13 skipping, but surprisingly, this mutation caused skipping of both exons 12 and 13.

In RT-PCR analysis using RNA from CHX-treated and CHX-untreated fibroblasts, we clearly showed that cDNA with skipping of exons 12 and 13 was the major transcript and was subjected to NMD. Both the cDNA with exon 13 skipping and the cDNA with exons 8–13 skipping should be minor and side transcripts because the former was not detected even in the CHX-treated condition and the latter is in-frame and had a relatively smaller amount than the major cDNA with skipping of exons 12 and 13 in the CHX-treated condition.

There are several reports of mutations at single-splice junctions that result in the skipping of two or more exons [Fang et al., 2001; Haire et al., 1997; Hayashida et al., 1994; Schneider et al., 1993; Takahara et al., 2002; Yamada et al., 2007]. The splicing order of introns can explain the events of aberrant splicing. Takahara et al. (2002) analyzed the molecular basis of skipping of exons 5 and 6 of COL5A1 due to a splice acceptor site of intron 5 mutation, by determination of the splicing order of introns 4, 5, and 6. They suggested that the acceptor-site mutation of intron 5 leads to the removal of the two downstream exons (exons 5 and 6), because those exons can be fused to a "single" exon, whereas the next downstream intron (intron 6) and the mutation-bearing intron (intron 4) remain in the transcript. Their finding could be applicable for a splice donor-site mutation, as the removal of the upstream intron creates a "single" exon that, if the next upstream intron is retained, allows

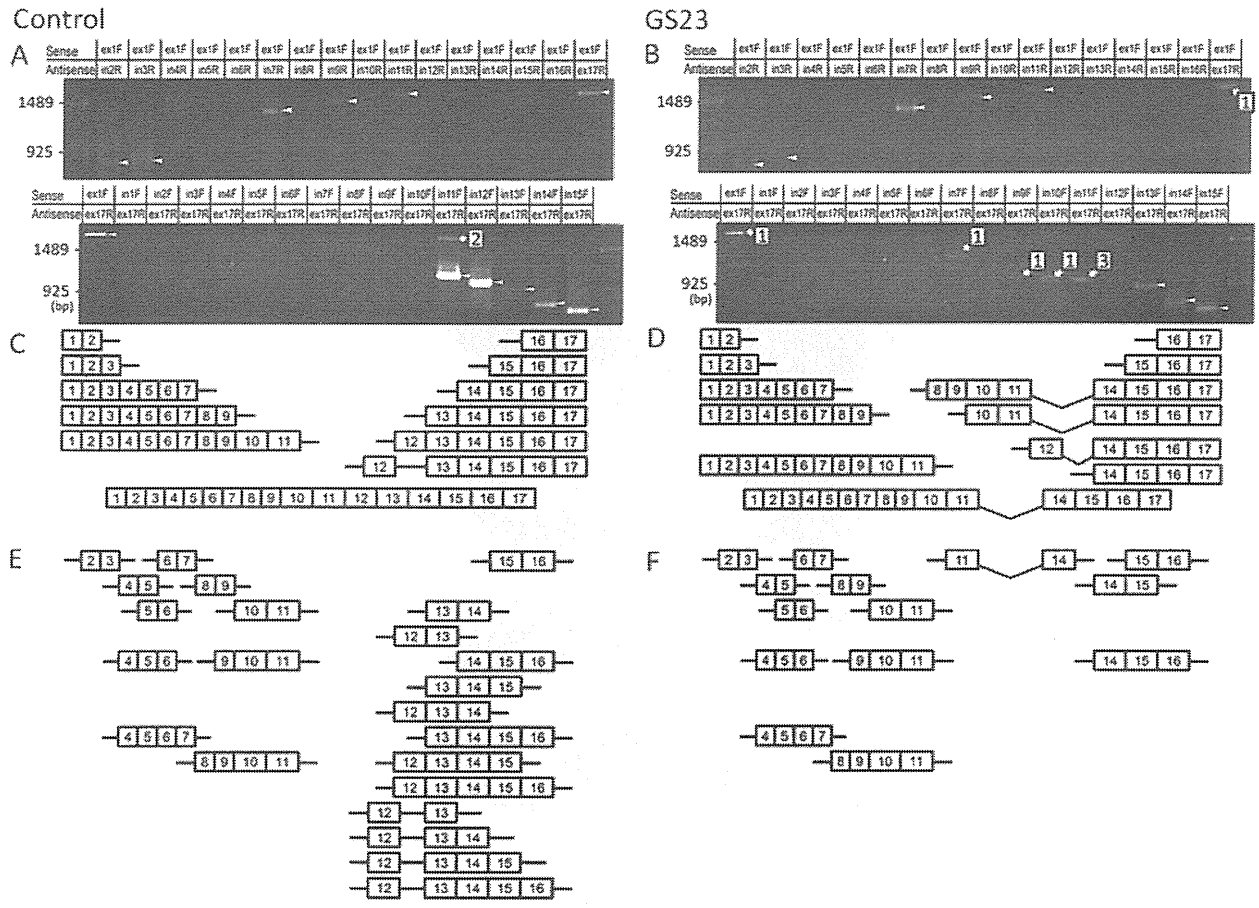

Figure 3. Detection of large SECRIs including exon 1 or exon 17. **A and B**: Detection of large SECRIs including exon 1 or exon 17. All fragments indicated by arrows and arrowheads were analyzed by direct sequencing. Fragments indicated by arrowhead without number had neither skipping of any exon nor retention of any intron. Fragments with arrow 1 had skipping of exons 12 and 13. A fragment with arrow 2 had a retention of intron 12. A fragment with arrow 3 had exon 13 skipping. **C and D**: Schematic presentations of SECRIs identified. **E and F**: All SECRIs flanked by introns which were detected (Supp. Fig. S1) are also schematically presented.

the skipping of the two exons upstream from the mutation site. We initially hypothesized that our case had the same molecular basis as described above. This outcome was actually reported in the case of a splice-donor site in the neurofibromatosis type 1 gene [Fang et al., 2001]. However, a SECRI comprising exons 12 and 13 was not detected in GS23 fibroblasts, suggesting that this pathway was not a major one.

Kessler et al. (1993) reported a method to determine the order of intron removal using RT-PCR in conjunction with appropriate combinations of intron and exon primers for any small pre-mRNA in vivo. Several reports determined the order of intron removal by this method [Attanasio et al., 2003; Schwarze et al., 1999]. Kessler's original method requires amplification spanning one intron; for example, amplification including whole intron 3 using 5′ primer in exon 3 and 3′ primer in intron 4. However, SCOT gene (gene symbol *OXCT1*) includes 17 exons and spans more than 150 kb. Because all introns except intron 12 were too long to amplify (1.2–33 kb), we could not determine a precise splicing order of *OXCT1* gene by this original method.

Our strategy involved (1) detection of a possible last intron to be spliced by amplification of SECRIs using combinations of sense primer in exon 1 and antisense primer in each intron and using combinations of antisense primer in the last exon and sense primer in each intron and (2) detection of any SECRIs comprising two, three, four, five, six sequential exons, and so on using intronic primers flanking adjacent exons or larger exon clusters (Fig. 3). This method is less definitive than the original method. Because the method relies on the analysis of steady-state RNA, we cannot rule out the possibility that some RT-PCR products may be side products or dead-end molecules in nuclear RNA. Moreover, the failure to identify a SECRI could be the consequence of at least two factors. The first would be retention of a larger upstream or downstream intron and the second would be the very rapid removal of the intron in which one primer was placed. Hence, even though we could construct several potential pathways of splicing, such pathways may not represent the major pathway. Even with the above limitations, our strategy may provide useful information on the molecular basis of splicing abnormality in a large gene such as SCOT gene.

We tried to assess order of removal of introns 11, 12, 13, and 14 in a dynamic fashion using actinomycin D treatment to halt transcription and with primer setting according to the Kessler's original method, as performed in several reports [Attanasio et al., 2003; Kessler et al., 1993; Schwarze et al., 1999]. As discussed above, because introns 11, 13, and 14 are too long to amplify intermediates including these introns, we could not determine the definite order of intron removal. However, these results could be best explained

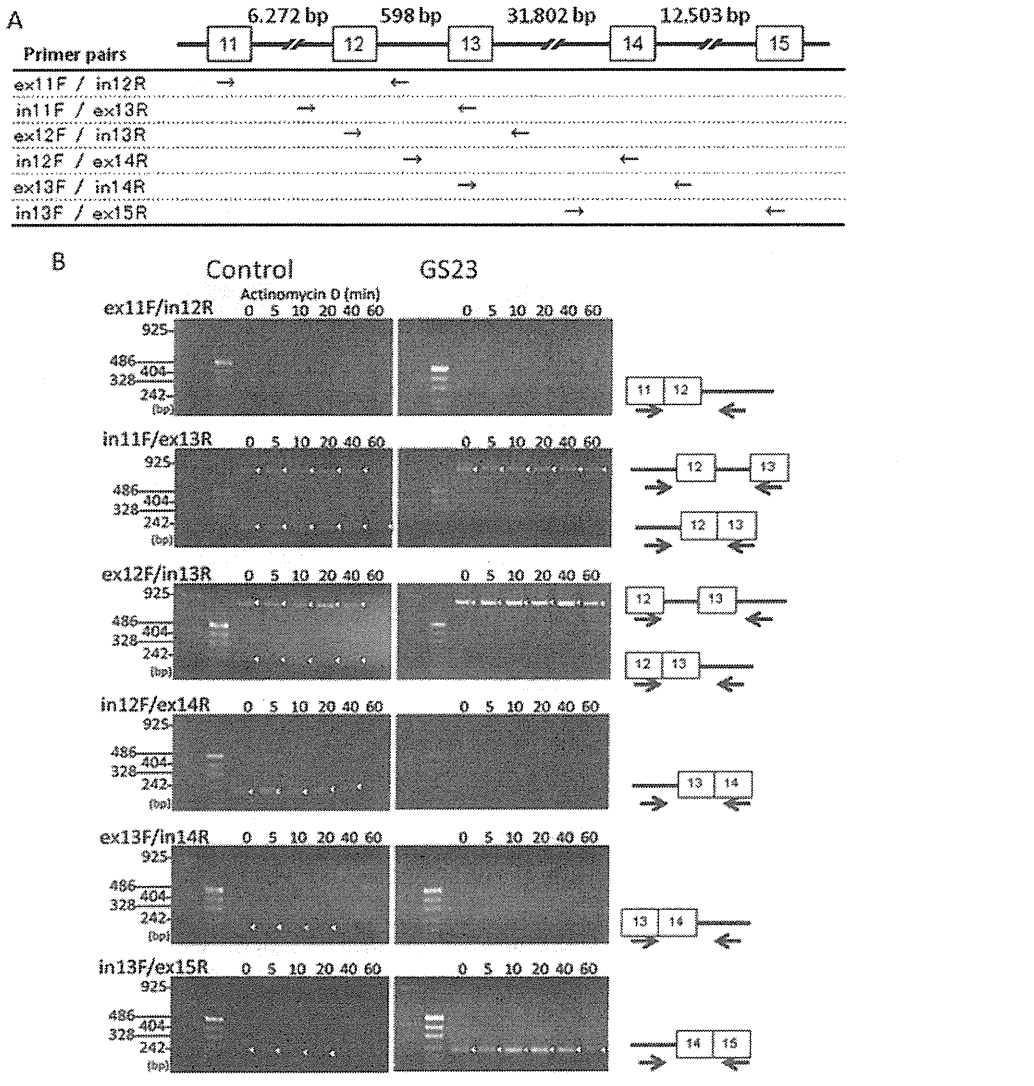

Figure 4. Analysis of intron removal around exons 11–14 using Actinomycin D. **A**: PCR primer combinations used for the analysis of intron removal. **B**: Total RNA was prepared from cultured fibroblasts after defined time intervals (0, 5, 10, 20, 40, and 60 min) of exposure to Actinomycin D, treated with DNase, reverse transcribed, amplified with indicated primer pairs, and electrophoresed on 2% agarose gels. Amplified fragments are indicated by arrowhead.

as follows: in control, intron 11 was the last intron to be spliced and intron 12 removal was also rather slow and occurred after intron 13 removal in the major pathway, although a minor pathway in which intron 12 splicing occurred before intron 13 was also present. In GS23, since intron 13 was mutated, retention of intron 13 occurred for a long time. This halt of intron13 splicing may result in intron 12 retention and intron 11 retention. This "splicing paralysis" [Schwarze et al. 1999] may be a molecular basis of two-exon skipping. This splicing paralysis could be solved by skipping of the whole intron 11–exon 12–intron 12–exon 13–mutated intron 13. The presence of all SECRIs detected, as shown in Figure 3, is consistent with the above explanation.

According to recent studies, splicing occurs during transcription (co-transcriptional splicing) and introns are removed in a general 5′–3′ order. However, as in our case, splicing does not always occur as a linear process starting at 5′ end of the primary transcript. Many different factors can influence the order of splicing of SCOT transcripts, including sequences at splice junctions, the length and sequences of introns, the sequences of adjacent exons, and RNA secondary structures. Supp. Table S2 summarizes the lengths of introns and exons in the SCOT transcript, and Shapiro and Senapathy's scores [Shapiro and Senapathy, 1987] of splice-site junctions. This analysis did not reveal a definitive factor that would explain the order of intron removal.

In summary, our study showed that (1) a single nucleotide substitution at the 5′ splice site of intron 13 (c.1248+5g>a) in GS23's fibroblasts causes skipping of exons 12 and 13 predominantly, that (2) the formation of SECRI comprising exon 12 and 13 was not the cause of skipping of exons 12 and 13 in GS23's fibroblasts, that (3) the mutation resulted in retention of intron 13, thus causing the retention of introns 12 and 11, and this "splicing paralysis" was the molecular basis of two-exon skipping.